

## Critical fields of Nb-Ta multilayers

P. R. Broussard\* and T. H. Geballe†

*Department of Applied Physics, Stanford University, Stanford, California 94305*

(Received 12 May 1986)

Nb-Ta multilayered films prepared by magnetron sputtering have been studied by critical-field measurements. We have examined the effects of substrate orientation and deposition temperature on the properties of the films. Three-dimensional to two-dimensional crossover is observed. For films with larger Nb layer thicknesses an additional transition in  $H_{c2||}$  at lower temperatures is observed which cannot be accounted for by the interfacial regions.

Since the original work on Nb-Ta multilayers by Durbin *et al.*,<sup>1,2</sup> it has been recognized that this system is the closest realization of a perfect metallic superlattice. Outside of the tunneling studies of Hertel *et al.*,<sup>3</sup> very little work has been done on the superconducting properties of the system. Encouraged by the work of Nb-Cu (Ref. 4) and Nb-Ti (Ref. 5), we have undertaken a study of the critical fields of the Nb-Ta system in order to examine the  $\dots S-S'-S-S' \dots$  multilayer, where  $S$  and  $S'$  denote superconductors. We have measured perpendicular and parallel critical fields and their angular dependence for several Nb-Ta multilayers. In addition we examine our results in light of the theoretical analysis of Biagi *et al.*<sup>6</sup>

The multilayers were prepared by magnetron sputtering from separate Nb and Ta sources onto different orientations of epitaxially polished sapphire substrates. The substrates were clamped to a heated platform that allowed us to vary the deposition temperature,  $T_D$ , from 600 to 800°C. The entire assembly was driven by a computer-controlled stepping motor which alternately moved the substrates through the separate deposition plasmas. The initial and final layers of the samples were tantalum, except for those used to study the dependence on substrate orientation and deposition temperature, which had niobium as the initial layer. The background pressure,  $P_B$ , was less than  $10^{-7}$  Torr with  $N_2$  and  $H_2$  being the predominant residual gases.  $H_2O$  was removed by a liquid-nitrogen-cooled Meissner trap. The argon pressure used during sputtering was 2 mTorr, and the deposition rates were typically 10–15 Å/sec.

The samples were initially characterized by x-ray diffraction and electrical resistivity measurements. Table I gives a relevant listing of the samples in this study. As in previous studies of the Nb-Ta system,<sup>1–3</sup> we find epitaxial growth onto the substrates and a single-crystal-type diffraction profile. However, we find that we can achieve this without the more stringent condition needed in the previous studies, i.e.,  $P_B < 10^{-8}$  Torr from the study by Durbin *et al.* or  $T_D > 800^\circ\text{C}$  from the study by Hertel *et al.*

The x-ray analysis on our samples was carried out with a four-circle Picker diffractometer and a Read camera<sup>7</sup> using Cu  $K\alpha$  radiation. The Read photographs demonstrate that the multilayers grow epitaxially on the sapphire substrates, with the sample reflections being only

slightly larger than the substrate reflections. Table I lists the rocking curve widths for the main Bragg peaks of the samples: (200) for the (1 $\bar{1}$ 02) sapphire, (110) for the (11 $\bar{2}$ 0) sapphire, and (222) for the (0001) sapphire. These are comparable to the study by Hertel but are somewhat larger than the work by Durbin.<sup>8</sup>

Figure 1 shows the diffractometer scans for sample 4 with  $\Lambda = 41$  Å deposited on (1 $\bar{1}$ 02) sapphire for both the low-angle satellites and the satellites around the main Bragg peak. The layered nature of the sample is clearly seen, with 6 orders of low-angle reflections and 4 sets of satellites around the (200) reflection. Analysis of the x-ray intensities of the low-angle reflections using the model of Kwo *et al.*<sup>9</sup> (after accounting for Lorentz-polarization,

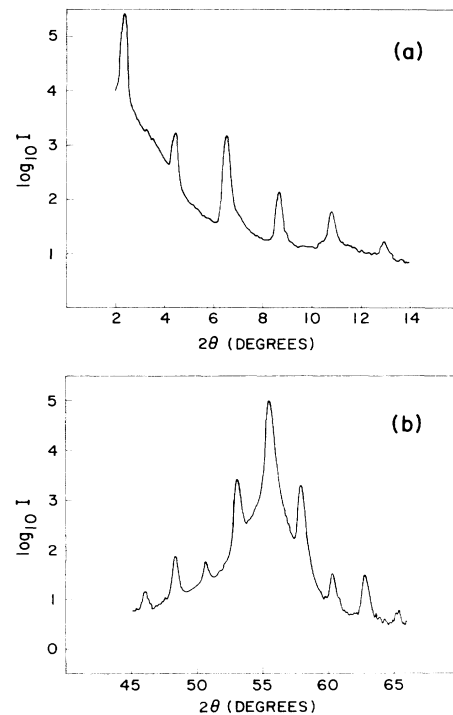


FIG. 1. X-ray scans along the growth direction on sample 4 with  $\Lambda = 41$  Å grown on (1 $\bar{1}$ 02) sapphire for (a) low-angle satellites and (b) around the (200) Bragg reflection for Nb and Ta.

TABLE I. Nb-Ta multilayer sample parameters. Here  $\Lambda = d_{\text{Nb}} + d_{\text{Ta}}$ , where  $d$  (in Å) is the ideal individual layer thickness of Nb and Ta, respectively (neglecting interfacial effects) and  $t$  is the total multilayer thickness. RRR is the residual resistivity ratio, and  $\Delta\omega$  is the rocking curve full width at half maximum.

Sample no.	Al <sub>2</sub> O <sub>3</sub>	$T_D$ (°C)	$\Lambda$ (Å)	$d_{\text{Nb}}/d_{\text{Ta}}$	$t$ (Å)	RRR	$l_0$ (Å)	$\Delta\omega$ (deg)
1a	1 $\bar{1}$ 02					4.70	100	0.57
1b	11 $\bar{2}$ 0	750	44	20/24	3960	4.14	87	0.58
1c	0001					4.56	99	0.42
2a	1 $\bar{1}$ 02					12.5	320	0.56
2b	11 $\bar{2}$ 0	750	193	85/108	9650	11.0	280	
2c	0001					13.2	340	
3	1 $\bar{1}$ 02	800	41	20.5/20.5	4100	5.00	110	0.44
4	1 $\bar{1}$ 02	750	41	20.5/20.5	4100	5.09	110	0.44
5	1 $\bar{1}$ 02	700	41	20.5/20.5	4100	5.07	110	0.55
6	1 $\bar{1}$ 02	650	41	20.5/20.5	4100	5.10	110	0.52
7	1 $\bar{1}$ 02	750	1010	490/520	5600	42.7	1200	0.46
8	1 $\bar{1}$ 02	750	780	290/490	5200	26.6	710	
9	1 $\bar{1}$ 02	750	575	98/477	5080	19.4	510	0.53

absorption, and Debye-Waller effects) indicates that the interface width (defined as the distance where the tantalum concentration changes from 10% to 90%) is  $\leq 8$  Å. This width is comparable to the study by Hertel, but is large than the value estimated by Durbin (4.5 Å). The reason for this difference may be due to the sputtering kinetics,<sup>10</sup> since in our sputtering geometry the (pressure)  $\times$  (distance) product is 15 cm mTorr, a very small value, and there is essentially no thermalization of the sputtered atoms.

The electrical resistivity of the samples was measured by the van de Pauw technique<sup>11</sup> with sample thickness measured by a depth profilometer. The results are listed in Table I. Using the value for the average renormalized Fermi velocity for niobium,<sup>12</sup> we can calculate a value of  $\rho l$  of 370 ( $\mu\Omega$  cm) Å, where  $\rho$  is the electrical resistivity in  $\mu\Omega$  cm and  $l$  is the electron mean free path in Å. This value is very close to that obtained by Mayadas *et al.*<sup>13</sup> and is of the same order as that assumed by Hertel [ $\approx 420$  ( $\mu\Omega$  cm) Å]. However it is much smaller than that used in the analysis of Durbin<sup>14</sup> [ $\approx 1200$  ( $\mu\Omega$  cm) Å], which was calculated using free-electron values for niobium and assuming 1 electron/atom in the conduction band. Our value was used to calculate  $l_0$ , the mean free path at low temperatures, shown in Table I. Even using this simple approach, we see that the mean free paths exceed  $\Lambda$  for all our samples. For comparison, homogeneous Nb<sub>0.5</sub>Ta<sub>0.5</sub> alloys prepared in our system have a low-temperature mean free path of  $\approx 40$  Å. The low temperature resistivity can also be a sensitive indication of the pressure of residual gases. For our pure niobium films, the resulting  $l_0$  is 4000 Å, of the order of the film thickness, indicating that scattering from surfaces is the predominant mechanism, not impurities. For pure tantalum films, on the other hand,  $l_0$  is a factor of 5 smaller. This value, however, agrees with that found by Durbin<sup>14</sup> for a pure tantalum

film (residual resistivity ratio of 25), indicating this smaller mean free path may be intrinsic to tantalum.

The samples were patterned with four leads in order to measure critical fields and were mounted onto a copper platform whose temperature was measured by a calibrated carbon glass thermometer. A current density of 30 A/cm<sup>2</sup> was used and the transition was determined by either sweeping temperature or magnetic field.  $H_{c2}(T)$  is defined consistently as  $R(H, T) = 0.5R_N$ , where  $R$  is the sample resistance and  $R_N$  is the normal-state resistance at low temperatures.

We first determined the effect of substrate orientation and deposition temperature on the film properties. Samples 1 and 2 were used to study the effect of orientation. These films have  $\Lambda = 44$  and 193 Å, respectively and were grown at 750°C. The x-ray and transport measurements show no clear preference for the best type of growth, as shown in Table I, although the (11 $\bar{2}$ 0) sapphire (or [110] growth) is uniformly poorer. This is different from our results on pure Nb films, which have a clear preference for (1 $\bar{1}$ 02) sapphire (or [100] growth) but agrees with the results for pure Ta films. The critical field results for  $\Lambda = 44$  Å, listed in Table II, show that the (11 $\bar{2}$ 0) sample, which has a higher  $\rho_0$  and a higher  $T_c$ , consequently has a higher perpendicular field slope. The Ginzburg-Landau coherence length for these samples as derived from the critical field slope is  $\xi_{\text{GL}\parallel}(0) \approx 190$  Å. The parallel

TABLE II. Critical-field dependence on substrate.

Al <sub>2</sub> O <sub>3</sub>	Samples 1a, 1b, and 1c; $\Lambda = 44$ Å.	
	$T_c$ (K)	$-H'_{c2\perp}(T_c)$ (Oe/K)
1 $\bar{1}$ 02	6.08	1410
11 $\bar{2}$ 0	6.18	1680
0001	6.04	1440

TABLE III. Critical-field data for samples 7, 8, and 9.

Sample no.	$d_{Ta}$ (Å)	$d_{Nb}$ (Å)	$T_c$ (K)	$-H'_{c2\perp}(T_c)$ (Oe/K)	$-H'_{c2\parallel}(T_c)$ (Oe/K)
7	520	490	7.69	484	765
8	490	290	6.95	560	736
9	477	98	5.57	508	596

critical-field slopes for these samples are all 1.6–1.7 times the perpendicular slopes which may indicate  $H_{c3}$  effects, as expected since these samples had Nb as the initial growth layer.

The effect of substrate temperature was examined with samples 3, 4, 5, and 6, which had  $\Lambda=41$  Å and were deposited on (1102) sapphires at temperatures of 650–800°C. From Table I, the variation in properties is even smaller than that between different substrates. The variation in critical-field properties was also small, with  $T_c=6.48\pm 0.03$  K and  $-dH_{c2\perp}/dT|_{T_c}=1380\pm 40$  Oe/K for all four samples.

Typical temperature dependence of the perpendicular critical field for these samples is shown in Fig. 2, where the data for samples 1 and 2 on (1102) sapphire is plotted. These samples show linear behavior far below  $t=1$  and cannot be fit within the context of the Werthamer, Helfand, Hohenberg, and Maki (WHHM) theory.<sup>15–17</sup> Attempts have been made to fit these results to the theory of Biagi, Kogan, and Clem for metallic multilayers; however, this is a theory valid for the dirty limit. The measure of how dirty a sample is, in the superconducting sense, is given by  $\lambda_{transport}$ , defined by

$$\lambda_{transport} = 0.882\xi_0/l_0,$$

where  $\xi_0$  is the BCS coherence length. For these samples,

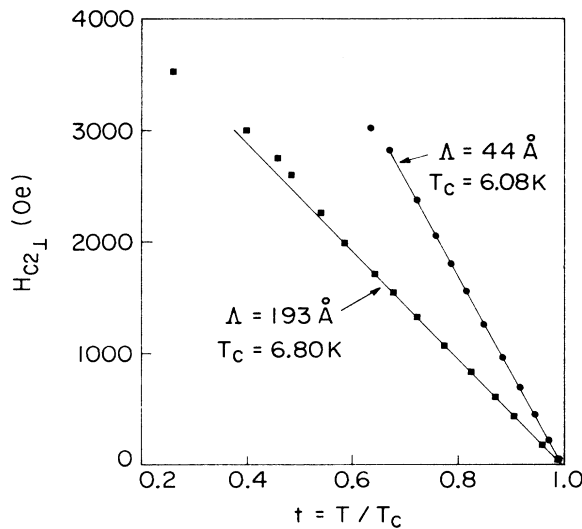


FIG. 2. Perpendicular upper-critical field versus reduced temperature for samples 1a ( $\Lambda=44$  Å) and 2a ( $\Lambda=193$  Å) grown on (1102) sapphire. The lines are a linear extrapolation of the data near  $t=1$ .

$\lambda_{transport} < 5$ , and the second-order corrections to the theory<sup>18</sup> are significant.

In order to look at dimensional crossover effects we deposited three samples (nos. 7, 8, and 9) with nearly constant Ta thickness ( $d_{Ta}\approx 500$  Å) and varying Nb thickness ( $d_{Nb}$  from 98 to 490 Å). These samples have large resistivity ratios and as such cannot be examined by the theory of Biagi *et al.*<sup>6</sup> The reduced perpendicular critical fields are shown in Fig. 3, and the relevant parameters are in Table III. Clearly the positive curvature increases as  $d_{Nb}$  increases in these samples, which may be due to the Nb layer becoming cleaner or a simple effect of the multilayering. Other explanations of positive curvature usually describe curvature close to  $t=1$ . In our work, the curvature is clearly below  $t=0.85$ . For comparison, Fig. 3 also shows the reduced field data for a Nb sample with a residual resistivity ratio (RRR) of 160,  $T_c=9.22$  K and a critical field slope of 512 Oe/K. The similarity between these data and the multilayer data strongly suggests that the positive curvature in the multilayers is an effect of the clean niobium layers. Obviously, any attempt to fit the data in this limit will require not only an extension towards the clean limit, but an inclusion of the effects of niobium's anisotropic Fermi surface.

The parallel critical-field data for the  $d_{Nb}=98$  Å sample are shown in Fig. 4. The data show behavior typical of a three-dimensional to two-dimensional (3D→2D) transition. We use the standard definitions of the coherence lengths of anisotropic superconductors,<sup>19</sup>

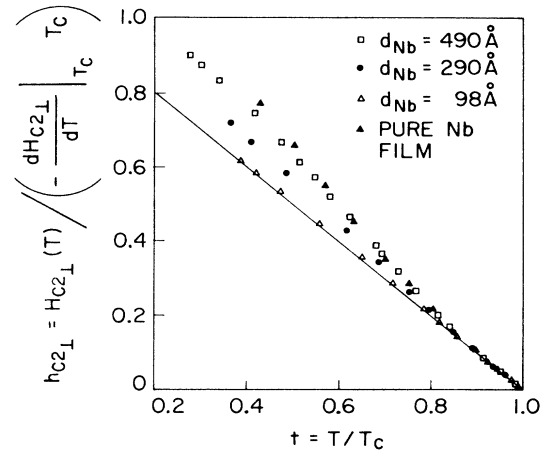


FIG. 3. Reduced perpendicular critical field versus reduced temperature for samples 7 ( $d_{Nb}=490$  Å), 8 ( $d_{Nb}=290$  Å), and 9 ( $d_{Nb}=98$  Å). Also included are the results for a pure Nb film with RRR equal to 160. The line is a linear extrapolation of the data near  $t=1$ .

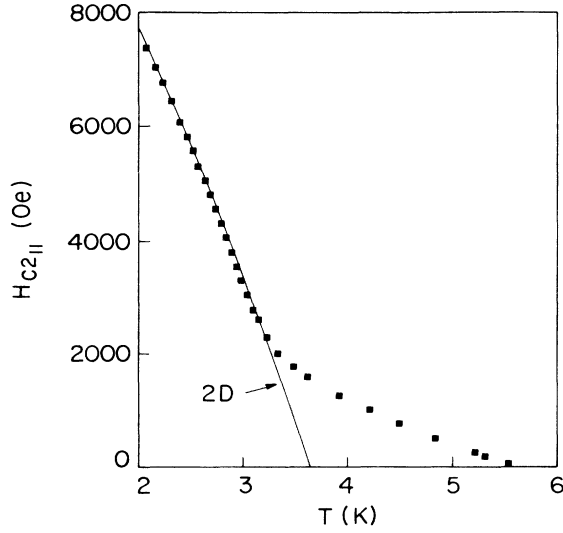


FIG. 4. Parallel upper-critical field versus temperature for sample 9 ( $d_{\text{Nb}} = 98 \text{ \AA}$ ). The line is a fit to the 2D equation (1).

$$\xi_{||} = \left[ \frac{\phi_0}{2\pi H_{c2||}} \right]^{1/2},$$

$$\xi_{\perp} = \left[ \frac{\phi_0 H_{c2\perp}}{2\pi H_{c2||}^2} \right]^{1/2},$$

where  $\phi_0$  is the flux constant. We can fit the 2D region of the data to the  $H_{c2||}$  equation<sup>20</sup> for a film with  $d_s$  less than both  $\xi_{\text{GL}}(T)$  and  $\lambda_{\text{GL}}(T)$ , where  $\lambda_{\text{GL}}(T)$  is the Ginzburg-Landau penetration depth,

$$H_{c2||} = \frac{\sqrt{12}\phi_0}{2\pi\xi_{||}d_s} \quad (1)$$

(for a 2D film) for  $2.1 \text{ K} < T < 2.8 \text{ K}$  as shown in Fig. 4. This analysis gives an effective superconducting thickness of  $86 \text{ \AA}$  and an effective transition temperature ( $T_c^*$ ) of  $3.6 \text{ K}$ . At this temperature  $\xi_{\perp} \approx 350 \text{ \AA}$ . Without a complete theory for the metallic multilayers in a parallel field, it is unclear what conclusions to draw from these numbers. Qualitatively one would expect a 3D $\rightarrow$ 2D transition for  $\xi_{\perp} > d_s$  when  $\xi_{\perp}$  goes from  $\gg d_N$  to  $\ll d_N$  (where  $d_s$  and  $d_N$  are the superconducting and normal layer thicknesses, respectively). In the theory of Klemm, Beasley, and Luther<sup>21</sup> for Josephson coupling the criterion is  $\xi_{\perp} = \Lambda/\sqrt{2}$ . For this sample the criterion would be  $406 \text{ \AA}$ , but one would not expect quantitative agreement for this theory, since in our case the coupling is through the proximity effect.

In Fig. 5 we plot the parallel critical field results for the  $d_{\text{Nb}} = 290 \text{ \AA}$  and  $490 \text{ \AA}$  samples. Whereas there was one transition for the  $98 \text{ \AA}$  sample, these samples have two transitions as the temperature decreases. We ascribe the first transition to a 3D $\rightarrow$ 2D crossover. To verify this, we examined the angular dependence of the critical field at different temperatures, shown in Fig. 6 for the  $290 \text{ \AA}$

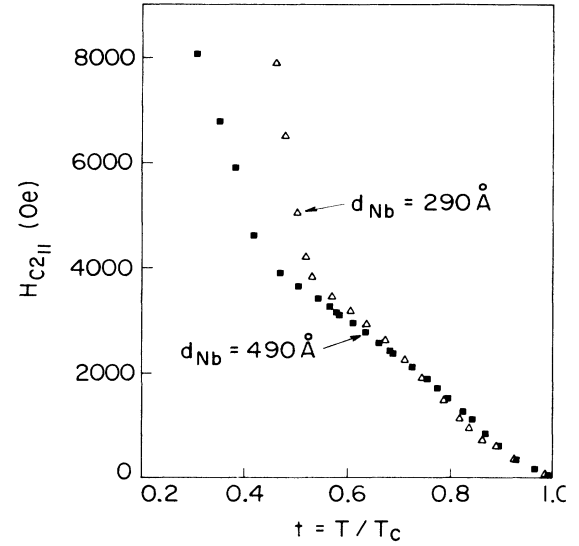


FIG. 5. Parallel upper-critical field versus reduced temperature for samples 7 ( $d_{\text{Nb}} = 490 \text{ \AA}$ ) and 8 ( $d_{\text{Nb}} = 290 \text{ \AA}$ ). Notice there are two transitions for each sample, with the 3D $\rightarrow$ 2D transition occurring at  $t = 0.8-0.9$ .

sample. For an anisotropic superconductor, the angular dependence would obey

$$H_{c2}(T, \theta) = \frac{H_{c2||}(T)}{[(m/M)\sin^2\theta + \cos^2\theta]^{1/2}}, \quad (2)$$

where

$$\frac{M}{m} = \left[ \frac{H_{c2||}(T)}{H_{c2\perp}(T)} \right]^2.$$

For a 2D film, the angular dependence obeys

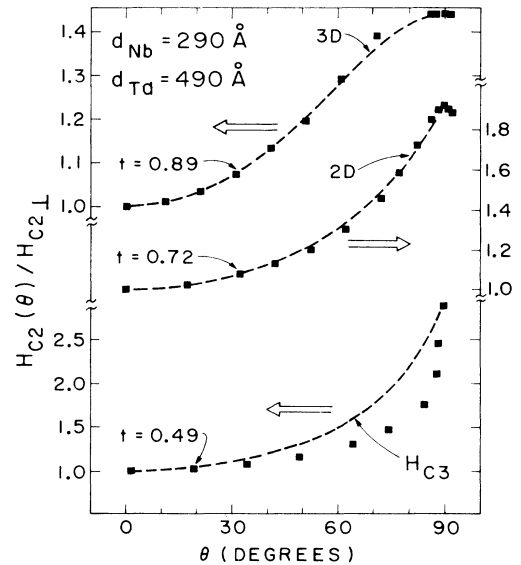


FIG. 6.  $H_{c2}(\theta)/H_{c2\perp}$  vs  $\theta$  for sample 8 ( $d_{\text{Nb}} = 290 \text{ \AA}$ ) at three different reduced temperatures. The dashed lines are fits to the angular dependence as follows:  $t = 0.89$  is fit to 3D equation (2),  $t = 0.72$  is fit to the 2D equation (3), and  $t = 0.49$  is fit to the result for surface state superconductivity ( $H_{c3}$ ).

$$\left| \frac{H_{c2}(T, \theta) \cos \theta}{H_{c2\perp}(T)} \right| + \left[ \frac{H_{c2}(T, \theta) \sin \theta}{H_{c2\parallel}(T)} \right]^2 = 1. \quad (3)$$

Above the transition ( $t = 0.89$ ), the data follow an anisotropic 3D fit with a zero slope at parallel field. Below the transition ( $t = 0.72$ ) the data fit the 2D equation with a cusplike behavior near parallel field. Therefore the first transition is to a state where the Nb layers are uncoupled and 2D-like.

At the lower transition ( $t = 0.49$ ),  $H_{c2\perp}$  has a sharp upturn with a local slope of  $\approx 6\text{--}10$  kOe/K. At this upturn,  $\xi_{\perp} \approx 200$  Å, and it would seem that the samples have gone through a 3D $\rightarrow$ 2D $\rightarrow$ low-temperature transition where  $\xi_{\perp}$  is less than all known length scales. However, the angular dependence in this region (shown in Fig. 6) shows a sharp cusp about the parallel field. The data cannot be fitted to either a 2D or surface-state angular dependence and would seem to indicate that the superconductivity is localized to layers of relatively high  $H_{c2}(T)$ . The rapid increase in the critical field near parallel field suggests that accurate alignment with these thin superconducting layers is critical. The interfacial regions of varying Nb-Ta composition, which should have a high  $H_{c2}$ , are one possibility. However, we know that the interfacial alloy region is less than 10 Å from x-ray measurements, and  $\xi_{\perp} \leq 200$  Å at these temperatures, so substantial averaging must be present. In addition, the NbTa alloys

typically have bulk upper critical-field slopes less than 2–3 kOe/K. Clearly the interfacial region is not the cause of this second transition. We cannot fully explain the nature of the superconductivity at these temperatures without a more complete theory that examines the parallel critical fields of a  $S$ - $S'$  multilayered system.

In conclusion, we find that for sputtered Nb-Ta multilayers there is less of an effect of substrate orientation on film quality than seen in the work of Durbin *et al.* For deposition temperatures between 650 and 800 °C, there is no variation in film properties, in contrast to the work of Hertel *et al.*  $H_{c2\perp}$  exhibits positive curvature in all samples, which we feel is due in part to the layering and in part to the intrinsic curvature in the  $H_{c2}$  of Nb. 3D $\rightarrow$ 2D crossover behavior has been observed, and for those cases when  $\xi_{\perp}$  decreases below all length scales a further transition occurs that results in a dramatic increase in  $H_{c2\perp}$ . The angular dependence at this transition is very sharply peaked and cannot be accounted for by the thin alloy interfacial layers, but may be due to the interplay between the two superconducting layers.

This work was supported principally by the U.S. Air Force Office of Scientific Research under Contract No. F49620-83-C0014. Samples were prepared and characterized at the Stanford University Center for Materials Research, supported by the National Science Foundation (NSF) Materials Research Laboratories (MRL) Program.

\*Present address: Naval Research Laboratory, Washington, D.C. 20375.

†Also at Bell Communications Research, Red Bank, NJ 07701.

<sup>1</sup>S. M. Durbin, J. E. Cunningham, M. E. Mochel, and C. P. Flynn, *J. Phys. F* **11**, 223 (1981).

<sup>2</sup>S. M. Durbin, J. E. Cunningham, and C. P. Flynn, *J. Phys. F* **12**, L75 (1982).

<sup>3</sup>G. Hertel, D. B. McWhan, and J. M. Rowell, in *Superconductivity in d- and f-Band Metals* (Kernforschungszentrum, Karlsruhe, 1982), p. 299.

<sup>4</sup>C. S. L. Chun, Guo-Guang Zheng, Jose L. Vincent, and Ivan K. Schuller, *Phys. Rev. B* **29**, 4915 (1984).

<sup>5</sup>Y. J. Quian, J. Q. Zheng, B. K. Sarma, H. Q. Yang, J. B. Ketterson, and J. E. Hilliard, *J. Low Temp. Phys.* **49**, 279 (1982).

<sup>6</sup>K. R. Biagi, V. G. Kogan, and J. R. Clem, *Phys. Rev. B* **32**, 7165 (1985).

<sup>7</sup>M. H. Read and D. H. Hensler, *Thin Solid Films* **10**, 123 (1972).

<sup>8</sup>It is difficult to compare to Durbin's values since he uses a linear method (Ref. 14) to remove instrumental broadening, instead of the quadrature method used here.

<sup>9</sup>J. Kwo, M. Gyorgy, D. B. McWhan, M. Hong, F. DiSalvo, C.

Vettier, and J. E. Bower, *Phys. Rev. Lett.* **55**, 1402 (1985).

<sup>10</sup>K. Myere, I. K. Schuller, and C. M. Falco, *J. Appl. Phys.* **52**, 5803 (1981).

<sup>11</sup>L. J. van der Pauw, *Phillips Res. Rep.* **13**, 1 (1958).

<sup>12</sup>H. R. Kerchner, D. K. Christen, and S. T. Sekula, *Phys. Rev. B* **24**, 1200 (1981).

<sup>13</sup>A. F. Mayadas, R. B. Laibowitz, and J. J. Cuomo, *J. Appl. Phys.* **43**, 1287 (1972).

<sup>14</sup>S. M. Durbin, Ph.D. dissertation, University of Illinois at Urbana-Champaign, 1983.

<sup>15</sup>N. R. Werthamer, E. Hefland, and P. C. Hohenberg, *Phys. Rev.* **147**, 295 (1965).

<sup>16</sup>K. Maki, *Physics* **1**, 21 (1964).

<sup>17</sup>K. Maki, *Physics* **1**, 127 (1964).

<sup>18</sup>V. Kogan, *Phys. Rev. B* **32**, 139 (1985).

<sup>19</sup>W. Lawrence and S. Doniach, in *Proceedings of the 12th International Conference on Low Temperature Physics, Kyoto, Japan, 1970*, edited by E. Kanada (Keigaku, Tokyo, 1971), p. 361.

<sup>20</sup>M. Tinkham, *Phys. Rev.* **129**, 2413 (1963).

<sup>21</sup>R. A. Klemm, M. R. Beasley, and A. Luther, *J. Low Temp. Phys.* **16**, 607 (1974).